Burns & Trauma, 2021, 9, tkab048
https://doi.org/10.1093/burnst/tkab048
Research Article

Research Article

Efficacy and safety of a dual-scan protocol for carbon dioxide laser in the treatment of split-thickness skin graft contraction in a red Duroc pig model

Jie Li[1], Sally Kiu-Huen Ng[2,3], Wenjing Xi[1], Zheng Zhang[1], Xiaodian Wang[1], Hua Li[1], Weijie Su[1,*], Jingyan Wang[4,*] and Yixin Zhang[1,*]

[1]Department of Plastic and Reconstructive Surgery, Ninth People's Hospital, Shanghai Jiao Tong University School of Medicine, Shanghai 200011, China, [2]Department of Plastic Surgery, Austin Health, Melbourne 3084, Australia, [3]Victorian Adult Burns Service, Alfred Health, Melbourne 3181, Australia and [4]Department of Plastic and Reconstructive Surgery, Xinhua Hospital, Shanghai Jiao Tong University School of Medicine, Shanghai 200092, China

*Correspondence. Weijie Su, Email: rosiewudi@163.com; Jingyan Wang, Email: jywdoctor@163.com; Yixin Zhang, Emai: zhangyixin6688@163.com

Received 5 May 2021; Revised 29 October 2021; Editorial decision 26 November 2021

Abstract

Background: Fractional CO_2 laser plays an important role in scar management post split-thickness skin graft by loosening the graft contracture and restoring the smoothness of the surface. However, the optimal treatment protocol remains unknown. This study applied a dual-scan protocol to achieve both releasing and ablation of contracted skin graft. We comprehensively describe this treatment method and compare the efficacy and safety between this dual-scan method and the conventional mono-scan mode.

Methods: A hypercontracted scar model after split-thickness skin grafting in red Duroc pigs was established. All scars meeting the inclusion criteria were randomly divided into four groups: high fluence–low density (HF–LD), low fluence–high density (LF–HD), combined group and control group. The energy per unit area was similar in the HF–LD and LF–HD groups. Two laser interventions were performed at a 6-week interval. The efficacy of the treatment was evaluated by objective measures of scar area, release rate, elasticity, thickness and flatness, while the safety was evaluated based on adverse reactions and melanin index. Collagen structure was observed histologically. The animals were followed up for a maximum of 126 days after modeling.

Results: A total of 28 contracted scars were included, 7 in each group. At 18 weeks postoperatively, the HF–LD and the combined groups showed significantly increased scar release rate ($p = 0.000$) and elasticity ($p = 0.036$) and decreased type I/III collagen ratio ($p = 0.002$) compared with the control and LF–HD groups. In terms of flatness, the combined group was significantly better than the HF–LD group for elevations <1 mm ($p = 0.019$). No significant skin side effects, pigmentation or scar thickness changes were observed at 18 weeks.

Conclusions: Dual-scan protocol could achieve superficial ablation and deep release of contracted split-thickness skin graft in a single treatment, with similar contraction release and texture improvement compared to a single deep scan. Its main advantage is to restore a smoother scar appearance. Adequate laser penetration was necessary for the release of contracted scars.

© The Author(s) 2021. Published by Oxford University Press.
This is an Open Access article distributed under the terms of the Creative Commons Attribution Non-Commercial License (http://creativecommons.org/licenses/by-nc/4.0/), which permits non-commercial re-use, distribution, and reproduction in any medium, provided the original work is properly cited.
For commercial re-use, please contact journals.permissions@oup.com

Downloaded from academic.oup.com/burnstrauma/article/doi/10.1093/burnst/tkab048/6490349 by guest on 14 October 2026

Key words: Skin graft contraction, Scar, Laser treatment, Fractional carbon dioxide laser

Highlights

- This study provides a comprehensive dual-scan protocol for the treatment of scar contractures with a fractional CO_2 laser.
- Objective assessments were used to compare the differences in efficacy and safety between the dual-scan and single-scan approaches.
- This dual-scan approach allows for 3D release and ablation of contractures in a single treatment.
- Adequate laser penetration has been validated as necessary to achieve scar release.

Background

Split-thickness skin graft is one of the most common reconstruction techniques to repair large skin defects after burns and trauma. Global data show that over 6 million patients receive skin grafting every year [1]. Contracture scarring due to graft contraction is one of the most common postsurgical complications. Scar hyperplasia or contracture affects more than 30% of patients, thereby affecting joint function [2,3]. Although skin graft contraction is a physiological response to reduce the wound area, it creates tension across adjacent tissues, causing cosmetic and functional impairment and affecting the quality of life of patients after skin grafting.

Physical therapy, represented by splinting and compression therapy, plays a significant role among traditional treatment measures; however, clinical evidence is limited. It has been suggested that continuous mechanical force to counteract the inward contraction of the skin grafts increases mechanical loading of the extracellular matrix and stimulates activity of myofibroblasts, limiting the effectiveness of external supports such as splints [4]. Physical therapy is only indicated for immature scarring and has limited effect on developed contractures [5,6]. Long-term brace wearing interferes with the patient's daily life and often results in low compliance.

Shumaker *et al*. first described the use of fractional CO_2 laser in the treatment of contracture scars in 2012. A fractional laser with parameters of 17.5–50 mJ and 5–15% coverage (Lumenis, Santa Clara, CA) was used to loosen contracture scars in the joint area and an ~12° increase in joint mobility was observed [7]. Since then, fractional CO_2 laser has been used for functional and cosmetic improvement of contracture scars and has become an essential complement to the traditional physical and surgical treatments [8,9]. However, the majority of the reported fractional laser applications in contracture scar treatments are case series [10,11]. Comparative studies between different protocols are lacking and the optimal fractional laser treatment protocol remains unknown. In a systematic review, Zuccaro *et al*. noted that the treatment parameters of the laser applied in most of the current studies depended on the clinical experience of the operator and detailed protocol information was not provided [12]. The available literature on fractional CO_2 treatment of contracture scars suggests that, to avoid excessive thermal damage, the density is correspondingly reduced as the laser energy increases [7,11], resulting in two main modes: high fluence–low density (HF–LD) and low fluence–high density (LF–HD) modes. The HF–LD mode uses a high-energy fractional laser to penetrate deep into the scar, with a lower coverage (1–5%), to achieve full-thickness releasing and remodeling. The LF–HD mode uses a low-energy fractional laser with increased coverage (>5%) to achieve superficial tissue ablation and improve the scar and surrounding tissue interface for a smoother scar appearance.

The treatment modality of the laser directly affects its efficacy. In skin graft contracture, both cosmetic and functional defects are present. Contraction of the graft in the joint area forms a contracture scar that affects joint function; contracture in the non-joint area causes a permanent reduction in surface area, resulting in a wrinkled scar appearance [13]. In this study, we describe a dual-scan protocol in detail and compare the effectiveness and safety between this dual-scan method and mono-scan modes by creating a contracted scar model on the back of red Duroc pigs.

Methods

Animal care and scar formation

All experimental operations were carried out and data were collected following the standards of the Animal Ethics Committee of the Shanghai Jiao Tong University School of Medicine. Two 3-month-old female red Duroc pigs (bodyweight 25–30 kg) were induced by general anesthesia with Telazol (Zoetis, Florham Park, NJ) and maintained by isoflurane. The skin was shaved on the back of the trunk and washed and disinfected using 2% chlorhexidine and 75% ethanol. Eight symmetrical 3 × 3 cm wounds were made with a scalpel on each side of the spine, and the entire layer of the skin was removed, reaching the superficial fascia and without damaging the subcutaneous fatty tissue. The wound edges were >3 cm apart. The removed skin was trimmed into a 0.026-inch split-thickness skin graft with a dermatome (Zimmer, Swindon, UK), and the graft was transplanted back to the original wound without meshing (Figure 1). Steriled gauze was soaked with 0.9% saline and the skin graft was packed and fixed by sutures. A transparent patch (3 M

Downloaded from academic.oup.com/burnstrauma/article/doi/10.1093/burnst/tkab048/6490349 by guest on 14 October 2026

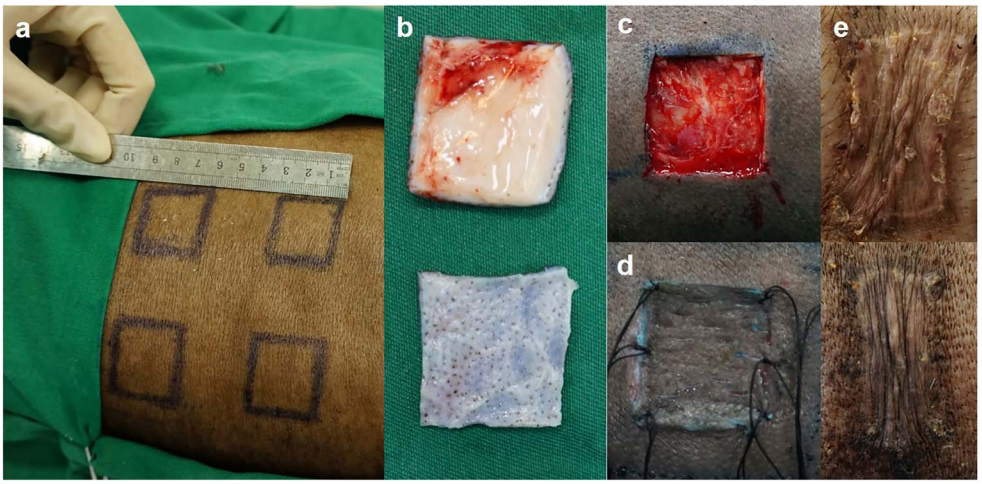

Figure 1. Animal modeling process. 3 × 3 cm wounds were made on each side of the spine (**a**); a 0.026-inch split-thickness skin graft was harvested (**b**); wound bed preparation (**c**); the graft transplanted back and fixed by sutures (**d**); scar appearance 6 weeks after modeling (**e**)

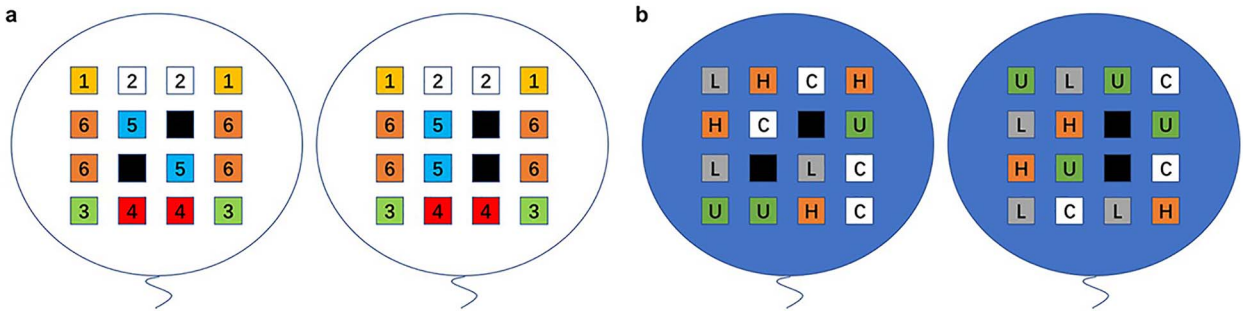

Figure 2. Randomization method. Scars that met the inclusion criteria were divided into six blocks based on the location. Black squares indicate grafts with <80% survival rate that were excluded (**a**). Final allocation results (**b**). 'H' refers to the HF–LD group, 'L' refers to the LF–HD group, 'C' refers to the control group and 'U' refers to the combined group

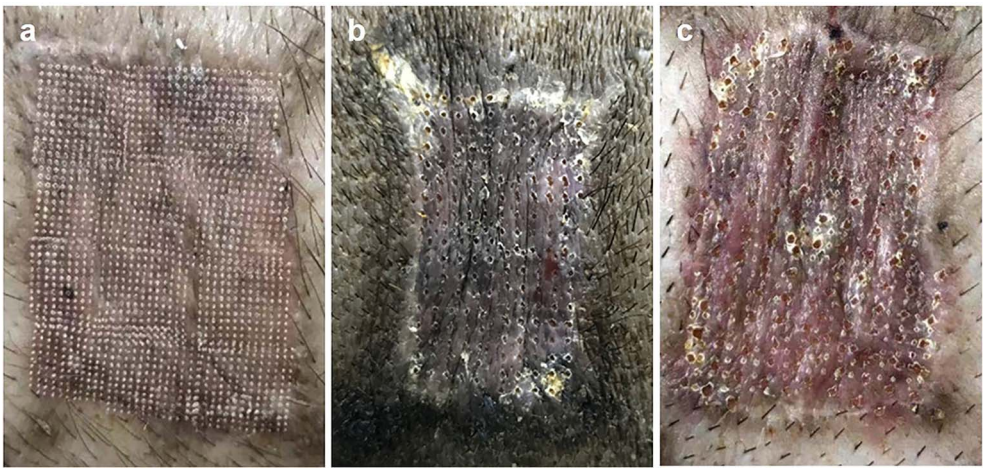

Figure 3. Scar appearance immediately after laser intervention. LF–HD group (**a**); HF–LD group (**b**); combined group (**c**). *HF–LD* high fluence–low density, *LF–HD* low fluence–high density

Healthcare, St. Paul, MN) was applied to the pig's back to protect the wound. The surface dressing, compression device and sutures were removed 10 days after grafting. After suture removal, the animals were bathed once a week with moisturizing soap to remove dead skin. The animals were kept indoors and protected from sun exposure. Skin grafts with survival rates >80% on day 10 were included for further intervention to avoid the impact of different skin graft survival rates on the scar contracture and final scar appearance.

Downloaded from academic.oup.com/burnstrauma/article/doi/10.1093/burnst/tkab048/6490349 by guest on 14 October 2026

Table 1. Time points for objective evaluations

Variable	Day 42	Day 63	Day 84	Day 105	Day 126
Biopsy for laser penetration	○				
Scar area	○	○	○	○	○
Release rate	○	○	○	○	○
Thickness	○	○	○	○	○
Elasticity	○				○
Melanin	○				○
Flatness					○
Biopsy					○

Laser intervention

The dual-scan protocol This treatment method consists of dual-scan steps. (1) First pass: laser microbeam penetration into the deep dermis (51–75% of the full-thickness), with 1–5% coverage, is used for deep contracture release. (2) Second pass: the laser beam penetrates to the epidermal junction or superficial dermis (<25%), with 5–10% coverage, for superficial scar ablation and resurfacing.

An ultrasound detector was used for scar thickness assessment before treatment. In uneven scar appearance, multiple points can be selected for scar thickness measurement, and the average thickness of the multiple points is used for further parameter selection.

We recommend compliance with the instructions provided by the manufacturer for the depth of laser penetration. For first-time used parameters, tissue biopsies can be used to clarify the depth of penetration.

Cohort and intervention Two interventions were performed, 42 and 84 days after modeling, with a treatment interval of 6 weeks. The skin was disinfected with 75% ethanol before the intervention. Fractional CO_2 laser (Alma Lasers, Caesarea, Israel) equipped with a Lite scan probe was used to treat the contracted scar. Scars that met the inclusion criteria were divided into six blocks (Figure 2a) based on the scar location, and randomization was performed within each block [14]. The random assignment of the intervention groups was performed using a random number scale generated by SAS software (Statistical Analysis System 9.4), which was created by researchers not involved in experimental operations prior to the start of data collection. Scars were randomized into four groups (Figure 2b) as follows. (1) HF–LD group: a mono-scan protocol, where the laser was set to an energy of 2800 mJ/pixel, a density 3 of 36 pixels/cm^2 and a total energy per unit area of 100.8 J/cm^2. (2) LF–HD group: a mono-scan protocol, where the laser was set to an energy of 960 mJ/pixel, a density 8 of 108 pixels/cm^2 and a total energy per unit area of 103.6 J/cm^2. (3) Combined group: a dual-depth scan protocol, where a HF–LD scan was performed first followed by an LF–HD scan; the total energy per unit area was 204.4 J/cm^2. (4) Control group: blank control, without any laser intervention.

The total energy per unit area was similar in the HF–LD and LF–HD groups (Figure 3). All of the treatment groups were cooled down with ice packs for 30 min after laser treatment, followed by aseptic dressings, and the dressings were changed every 3 days until the wounds healed.

Penetration percentage and ablation coverage At postoperative week 6, immediately after the laser intervention, three randomly selected scars in the HF–LD and LF–HD groups were subjected to tissue biopsy (6 mm). All biopsies collected were positioned near but not on the scar edge to reduce any influence on scar contraction. Tissues were embedded in Optimal Cutting Temperature (OCT) resin, frozen, cryosectioned and stained with hemoglobin and eosin (H&E). Measurements of microthermal zones were performed using Image J software following previous publications [15]. At least 10 unique wells from each group were measured. Penetration percentage and coverage were calculated as follows: penetration percentage = laser ablation depth/scar thickness × 100%; coverage = single-pixel ablation size × number of pixels/area × 100%.

Outcome assessment

Data were collected at 6, 9, 12, 15 and 18 weeks postoperatively and follow-up continued until 18 weeks after modeling (Table 1).

Primary indicator: scar release rate Digital photographs of the scar were collected at follow-up (Canon 750D, Japan). ImageJ software was used for the measurement of the scar area. The scar area before the laser intervention and at 6 weeks post skin grafting was taken as S_0 and the scar area was evaluated at each follow-up as S_t. The scar release rate was calculated as follows: $(S_t - S_0)/S_0 \times 100\%$.

Secondary indicators

Scar thickness Scar thickness was detected by color Doppler ultrasound detector (M7, MindRay Co., Shenzhen, China).

Scar elasticity Scar elasticity was measured by a multi-probe skin detector (Cutometer MPA580, Germany) at a room temperature of 20–22°C and relative humidity of 45–55%. A 4-mm-diameter suction probe was used with the time-strain mode of continuous negative pressure (mode 1). The suction force size was 500 mbar (50 kPa), the negative pressure lasted

Downloaded from academic.oup.com/burnstrauma/article/doi/10.1093/burnst/tkab048/6490349 by guest on 14 October 2026

Table 2. Scar characteristics before intervention at 6 weeks after grafting

Variable	HF–LD group	LF–HD group	Combined group	Control group	*P* value
Scar area (mm^2)	678.56 ± 130.78	697.95 ± 170.05	691.86 ± 129.57	683.66 ± 134.15	0.995
Thickness (mm)	0.34 ± 0.06	0.34 ± 0.06	0.32 ± 0.06	0.33 ± 0.06	0.892
Elasticity (R_2)	0.77 ± 0.17	0.80 ± 0.21	0.78 ± 0.12	0.79 ± 0.14	0.984
Melanin	869.43 ± 12.34	867.29 ± 10.89	864.57 ± 8.38	871.43 ± 12.93	0.702

HF–LD high fluence–low density, *LF–HD* low fluence–high density

Table 3. Average treatment parameters

Variables	HF–LD group	LF–HD group
Ablation depth (mm)	2.05 ± 0.08	0.78 ± 0.04
Penetration (%)	60.89 ± 3.03	21.57 ± 2.06
Spot diameter (μm)	311.31 ± 46.34	300.74 ± 5.54
Coverage (%)	2.78 ± 0.84	7.67 ± 0.28

Data are presented as mean ± standard deviation. *HF–LD* high fluence–low density, *LF–HD* low fluence–high density

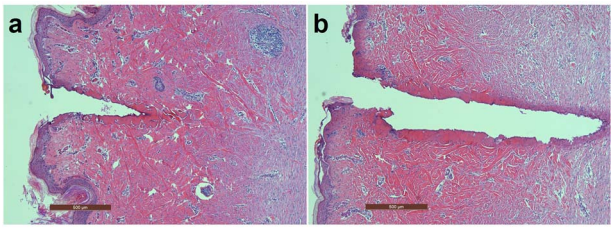

Figure 4. H&E staining results for laser penetration (scale bar: 500 μm). Biopsy from LF–HD group (**a**); HF–LD group (**b**). *HF–LD* high fluence–low density, *LF–HD* low fluence–high density, *H&E* hemoglobin and eosin

for 2 s, relaxation was 2 s, each site was tested for three cycles and the total values were averaged.

Melanin index Melanin index was measured by colorimetry (Dermacatch, Colorix, Neuchatel, Switzerland).

Scar flatness The scar flatness was defined as the volume of protrusion above the skin surface and was measured using an Antera3D camera (Miravex Limited, Ireland). The protrusion mode was selected with two different filters. The large filter (<3 mm) was used to detect V_L isometric elevations thinner than 3 mm; the small (<1 mm) filter was used to detect small elevations V_S thinner than 1 mm.

Adverse reactions Side effects after laser treatment were observed and recorded, including delayed healing, pigmentation changes, new scar formation, persistent erythema, *etc*.

Histological examination

At week 18, tissue biopsies (6 mm in diameter) were obtained and H&E staining results were used to observe the general tissue structure. Sirius red staining results were used to analyze the collagen fiber type and structure. In the polarized light field, orange-red fibers represented type I collagen and green fibers represented type III collagen. Image Pro Plus software was used for quantitative analysis of type I and III collagen, and the type I to type III collagen ratio was calculated for further analysis.

Statistical analysis

SPSS software, version 19 (IBM Company, Armonk, NY) and R software (version 4.0.2; R Foundation for Statistical Computing, Vienna, Austria) with nlme and lsmeans packages were used for statistical analysis. Data were tested for normality using the Shapiro–Wilk test and described by mean ± standard deviation. For data evaluated on multiple time points, mixed-effects models were used to exclude confounding factors of time and interaction. Tukey's test was used for the *post hoc* test between groups. One-way Analysis of Variance (ANOVA) was used to compare differences among groups at the same time point. Detailed data and statistics of the randomization result are available as online supplementary material (Appendix A) P value <0.05 (two-tailed) was considered statistically significant.

Results

Scar characteristics

In this study, a total of 32 grafts were modeled. At day 10 postoperatively, 28 grafts with a survival rate of >80% were included, resulting in a modeling success rate of 87.5%. All of the scars were randomly divided into four groups, seven in each group. Before intervention (6 weeks after grafting) there were no significant differences in the scar area, thickness, elasticity and melanin index between the groups ($p > 0.05$) (Table 2).

Penetration percentage and coverage

According to the histological examination, the laser penetrated 21.57% of the full thickness with a coverage of 7.67% in the LF–HD group and 60.89% in the HF–LD group with a coverage of 2.78% (Table 3 and Figure 4).

Scar appearance and contraction

At 18 weeks postoperatively, a smoother scar appearance was observed in the combined group from a general view (Figure 5). However, from the objective data, there was no statistical difference in scar area between the four groups ($p = 0.786$). From week 12, the release rate was significantly higher in the combined groups than in the

Downloaded from academic.oup.com/burnstrauma/article/doi/10.1093/burnst/tkab048/6490349 by guest on 14 October 2026

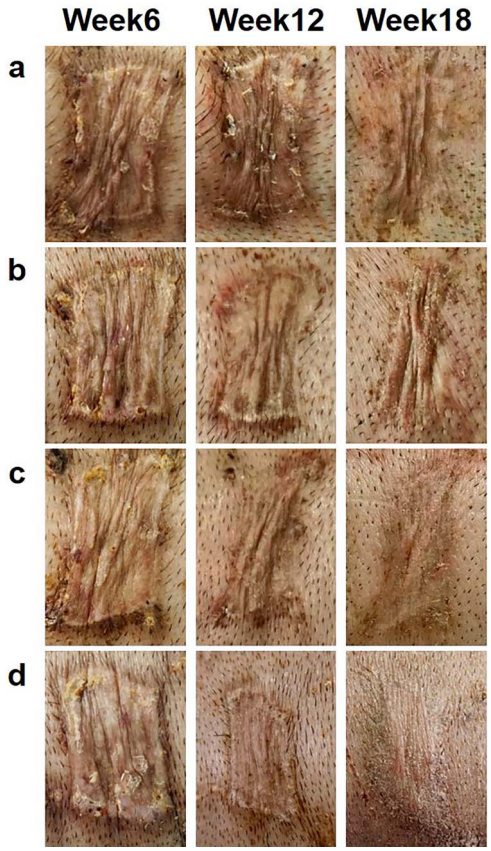

Figure 5. General view of scar appearance. Control group (**a**); LF–HD group (**b**); HF–LD group (**c**); combined group (**d**). *HF–LD* high fluence–low density, *LF–HD* low fluence–high density

control group (Figure 6a, b). At week 18, the release rate was 15.23 ± 7.81% in the HF-LD group and 16.37 ± 5.02% in the combined group, significantly higher than those in the LF-HD group (−0.72 ± 6.46%) and the control group (0.53 ± 6.09%) ($p = 0.000$).

Secondary indicators

Scar thickness

At 18 weeks of follow-up, there was no statistically significant difference in scar thickness among the four groups ($p = 0.104$) (Figure 6c).

Scar elasticity

Cutometer MPA 580, a skin elasticity detector, is based on the principle of mechanical measurement and suction. Parameters including $R_0 - R_9$ were measured. Among them, R_2 (U_a/U_f) refers to the total elastic-plasticity of the resilient part/the total elastic-plasticity of the stretched part, reflecting the total resilience of the scar skin, and is commonly used as an evaluation index for skin elasticity. Values closer to 1 indicated better skin elasticity.

At 18 weeks, the R_2 value was 0.83 ± 0.17 in the HF–LD group and 0.82 ± 0.16 in the combined group, which was significantly higher than that in the control group 0.57 ± 0.18 ($p = 0.036$) (Figure 6d). There was no statistically significant difference between the LF–HD group compared to the control group ($p = 0.997$).

Melanin index

At 18 weeks, melanin values were not statistically different among the four groups ($p = 0.475$) (Figure 6e).

Scar flatness

At 18 weeks, the V_L value of the combined group was significantly lower than that of the control group for the large elevations within the height of 3 mm ($p = 0.013$) (Figure 7a, b). For small elevations thinner than 1 mm, the V_S value of the combined group was significantly lower than that of the HF–LD group ($p = 0.019$) and the control group ($p = 0.025$), but there was no significant difference compared with the LF–HD group ($p = 0.256$) (Figure 7c, d).

Adverse reactions

No significant skin side effects were observed in each treatment group.

Histological results

From the H&E staining results, collagen arrangement was disordered in the control group. In contrast, the whole layer of the scar in the HF–LD and combined groups showed a more orderly and parallel arrangement of the collagen structure; the restored dermal papillae were visible in the superficial layer of the LF–HD group, but the deep layer still maintained a stale and similar appearance to that of the control group (Figure 8). From the results of Sirius red staining, the type I/III collagen ratio was significantly lower in the HF–LD and combined groups compared with the control group ($p = 0.002$); the LF–HD group showed no significant difference compared with the control group ($p = 0.979$) (Figure 9).

Discussion

Due to the prevalence of postoperative skin graft contraction, clinicians often avoid using split-thickness skin grafts in areas with high cosmetic and functional requirements. The functional and cosmetic differences can be improved by increasing graft thickness; however, this is often accompanied by a greater risk of donor area complications [16]. The reduction of scar contraction and uneven scar appearance is crucial for improving the patients' quality of life. Fractional laser is an effective contracture scar treatment [17]; the choice of treatment parameters and protocol of fractional laser determines its efficacy. To our knowledge, this is the first published study comparing the effectiveness and safety of mono-scan and dual-scan techniques of the fractional laser in contracted scar treatment. Additionally, we compared the effect of HF–LD and LF–HD modes in a mono-scan protocol for contracture scar treatment at similar unit area energy.

Downloaded from academic.oup.com/burnstrauma/article/doi/10.1093/burnst/tkab048/6490349 by guest on 14 October 2026

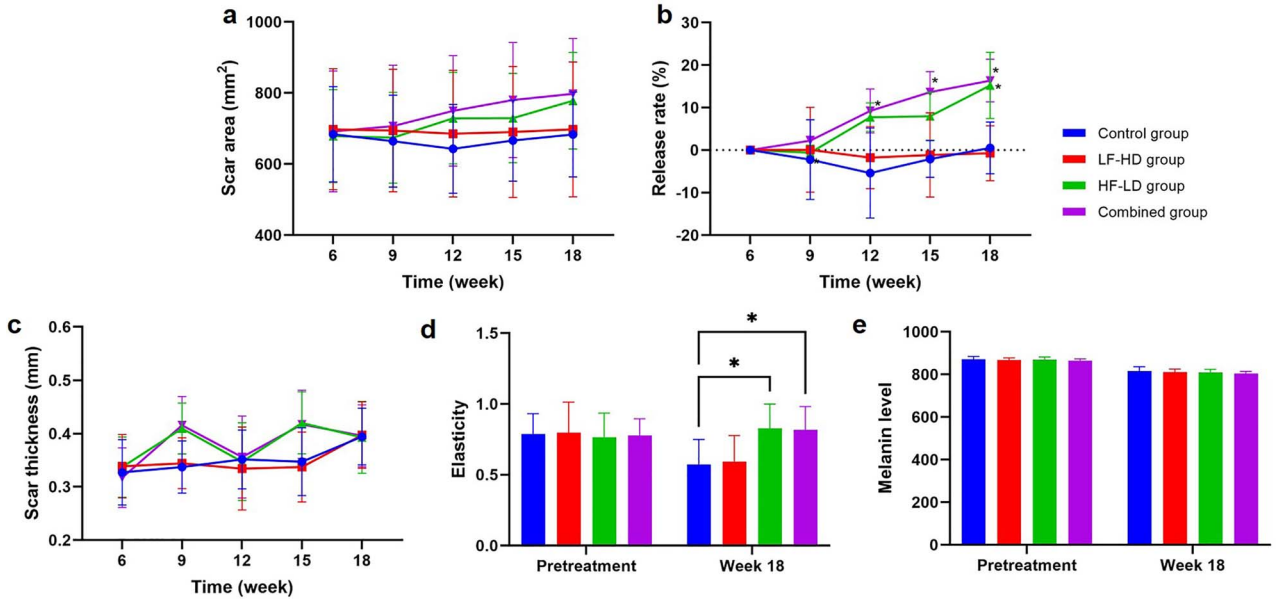

Figure 6. Scar area (**a**), release rate (**b**) and scar thickness (**c**) as a function of time and treatment. Assessment of scar elasticity (**d**) and melanin index (**e**) at weeks 6 and 18. *Indicates a statistical difference compared with the control group ($p < 0.05$). *HF–LD* high fluence–low density, *LF–HD* low fluence–high density

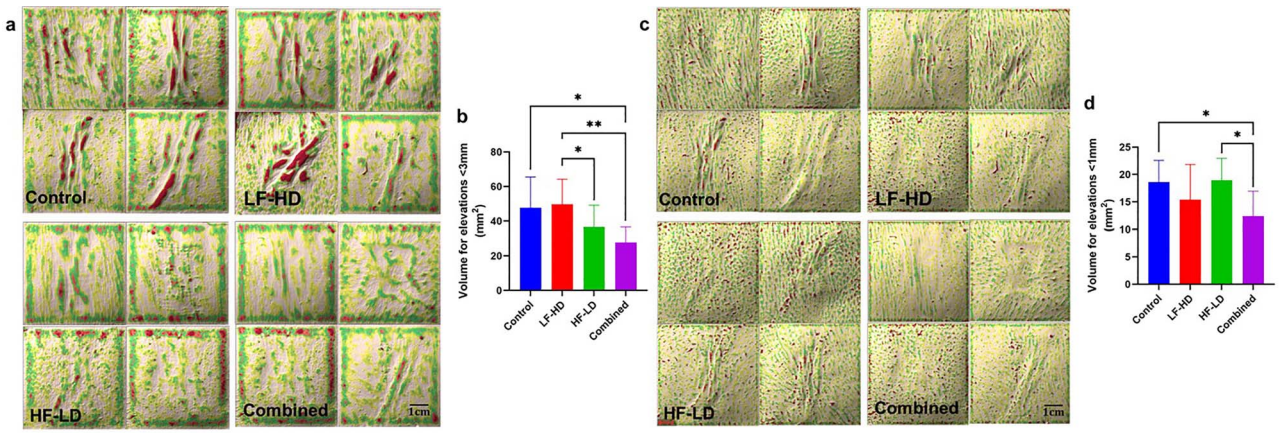

Figure 7. Assessment of surface flatness at week 18 (scale bar: 1 cm). Antera 3D image showing large elevations thinner than 3 mm (**a**); V_L value in each group (**b**); Antera 3D image for small elevations thinner than 1 mm (**c**); V_S value in each group (**d**). *$p < 0.05$, **$p < 0.01$. *HF–LD* high fluence–low density, *LF–HD* low fluence–high density

Most previous studies have standardized laser parameters to a defined range of values without clearly relating them to the thickness of the scar, which poses two difficulties: (1) using the same laser parameter for scars of different thicknesses and contracture extent limits the laser performance and may lead to entirely different treatment outcomes [18]; (2) different brands of commercial machines make conversion and equivalence between parameters impossible, reducing the generalizability of laser treatment protocols. Anderson *et al*. published a consensus on laser treatment of traumatic scars in 2014, suggesting that the laser penetration proportional to scar thickness should be a more critically standardized parameter [19].

The dual-scan protocol with fractional CO_2 laser has been used in the treatment of hypertrophic scars, acne scars and facial rejuvenation [20–23]. Hultman *et al*. applied a dual-depth scan technique in 147 cases of post-burn scars and concluded that the texture, thickness and elasticity of the scar were improved by remodeling and resurfacing at different depths to achieve an improved overall appearance of the scar [24]. However, past studies did not describe the penetration depth of the dual-scan and lacked a comparison of the dual-scan and mono-scan modes in terms of treatment efficiency and safety. This research comprehensively describes the treatment layer of the dual-scan protocol. In the deep scan, the depth of laser penetration was 51–75%. In clinical practice, some physicians believe that a laser penetration close to the full-thickness could lead to better treatment results, but due to a lack of comparative studies, no uniform conclusion has been reached on the optimal laser penetration depth.

Downloaded from academic.oup.com/burnstrauma/article/doi/10.1093/burnst/tkab048/6490349 by guest on 14 October 2026

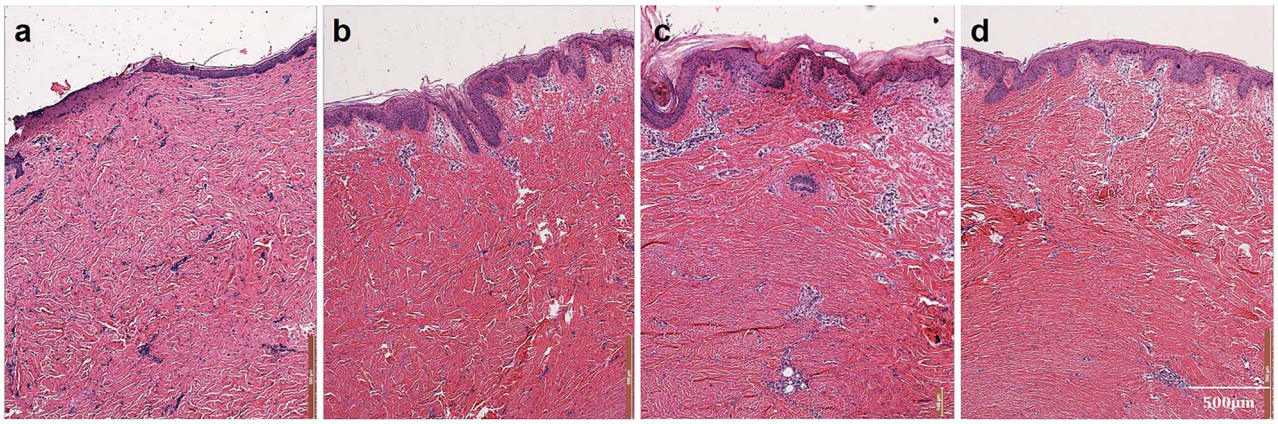

Figure 8. The histological results of H&E staining (×40) at week 18 (scale bar: 500 μm). Control group (**a**); LF-HD group (**b**); HF-LD group (**c**); combined group (**d**). *HF–LD* high fluence–low density, *LF–HD* low fluence–high density, *H&E* hemoglobin and eosin

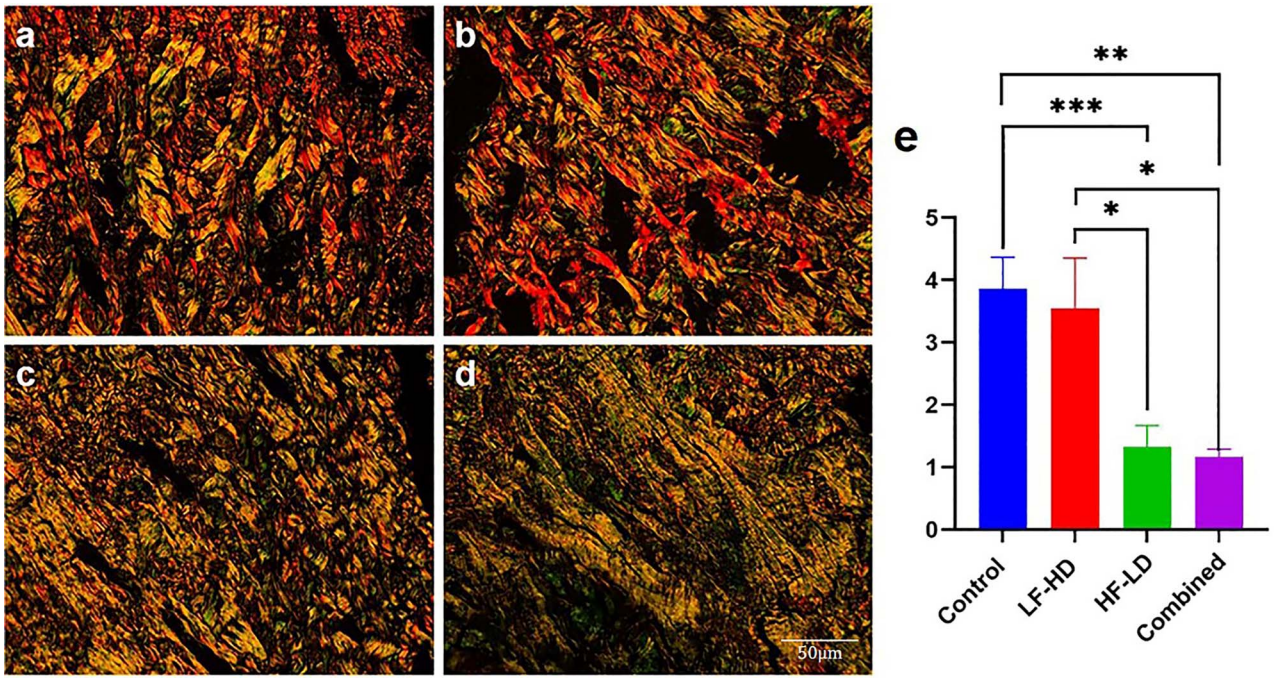

Figure 9. Polarized microscopy images (scale bar: 50 μm, ×200). Collagen fibers are highly birefringent, with type I collagen fibers (Col1) appearing orange-red and type III collagen fibers (Col3) appearing green. Control group (**a**); LF–HD group (**b**); HF–LD group (**c**); combined group (**d**); ratio of Col1/Col3 (**e**). $^{***}p < 0.001$, $^{**}p < 0.01$, $^{*}p < 0.05$. *HF–LD* high fluence–low density, *LF–HD* low fluence–high density

The parameter settings for this study were referenced from a retrospective study by Issler-Fisher *et al*. They compared the treatment efficiency of different laser penetration and concluded that a penetration of 51–75% achieved the maximum scar reduction [25]. In the superficial scan, we used a depth of <25% full-thickness. This is because previous studies of skin graft treatment reported the regeneration of the dermal papillae as a characteristic change of superficial fractional CO_2 laser treatment to achieve surface smoothness and improve skin texture [26]. Therefore, the depth of the superficial scan was used to break through the epidermis into the superficial dermis, and accordingly, the superficial coverage was adjusted to 5–10%. The treatment parameters used in this study were 60.89% penetration in the deep scan with 2.78% coverage for achieving full dermal collagen release and rearrangement, and 21.57% penetration in the superficial scan with 7.67% coverage for resurfacing and smoothing improvement, following the dual-scan protocol we proposed.

The release rate and elasticity of contracture scars at 18 weeks postoperation were significantly better in the HF–LD and the combined groups than in the control and the LF–HD groups, and no significant difference was seen between the HF–LD and combined groups. This suggests that adequate laser penetration depth is a decisive factor in achieving contracture scar release and functional recovery, and that increased coverage does not result in effective scar release

Downloaded from academic.oup.com/burnstrauma/article/doi/10.1093/burnst/tkab048/6490349 by guest on 14 October 2026

when laser penetration is insufficient. The rationale for fractional CO_2 laser release of scar contracture include (1) vaporization to remove thickened and disordered abnormal collagen, providing space for neocollagen [27]; (2) increasing tissue elasticity and inducing fine collagen production, mainly type III collagen [28]; (3) contributing to fibroblast apoptosis [29]; and (4) attenuating scar-related proinflammatory cytokine secretion in tissues [15]. The laser in HF–LD and combined groups can penetrate into the deeper half of scars, vaporize and remodel the full thickness, which is necessary for releasing contracture scars. The histological results also supported this view. From the H&E staining results, finer, ordered, parallel-aligned collagen structures were observed in the whole layer of the scar in the HF–LD and combined groups compared with the control group, while the collagen arrangement in the deeper layers of the scar remained disorganized in the LF–HD group.

Regarding scar flatness, at 18 weeks after surgery, for significant elevation above the skin surface (up to 3 mm), the HF–LD and combined groups were significantly better than the LF–HD group. However, data on thickness of <1 mm in height showed that the combined group was significantly more effective than the HF–LD and control groups, and there was no significant difference from the LF–HD group; this suggests that adequate tissue penetration depth is more critical for the improvement of large folds and that increased coverage improves smoothness. The dual-scan mode of the combined group showed advantages in flattening small elevations on the scar surface. Higher densities have been suggested for photoaging skin treatments to reduce wrinkles and improve skin smoothness [30]. Datz *et al*. used a high-density treatment mode to treat full-thickness skin grafts; scar and surrounding tissue adaptation increased, and a flatter scar appearance and uniform pigment distribution were observed [31]. In this study, the combined group allowed for superficial ablation and helped the fading of small elevation on the scar surface.

Inflammatory hyperpigmentation and new scar formation are considered the most common adverse effects of excessive photothermal damage after fractional laser treatment [26,32]. In this study, no significant pigmentation changes or other skin side effects were observed in the combined group during the follow-up. From the objective data, the thickness of the scar and the melanin index at 18 weeks after the procedure were not significantly different between the study groups. A total of two fractional laser interventions were performed in this study, and a transient increase in thickness was found in the HF–LD and combined groups 3 weeks after each intervention without causing a significant difference.

Reviewing the literature, major side effects of dual-scan protocol include post-treatment edema, erythema and short-term inflammatory hyperpigmentation (≤3 months) [33–35], whereas no long-term or permanent side effects have been reported. The study by Cameli *et al*. compared dual-scan and mono-scan protocols in acne scar treatment and found better treatment results without increasing skin side effects [36]. The thermal effect of multiple passes with CO_2 laser was reported by Fitzpatrick *et al*. [37]. Their work showed that residual thermal necrosis remained well controlled for passes 1 to 3, which are commonly used clinically for skin resurfacing. While each pulse interacts independently with the tissue, the heated layer has time to cool. No significant thermal diffusion occurs during the pulse due to the short pulse width. In this study, two independent pulses were performed, with sufficient cooling time between pulses. Cold packs immediately after treatment also reduced residual thermal damage. The penetration depth using the dual-scan protocol in this study was <75% and nearly 90% of the epidermis was preserved to allow for rapid tissue repair. These measures increased the safety of the dual-scan treatment in this study. In clinical application, the patient's skin type, location of the scar, maturity and sun exposure may affect the treatment outcome [25]. Further prospective clinical trials with large samples should be conducted for a more accurate safety assessment.

In general, our results showed that adequate tissue penetration was necessary for the recovery of contracted scars. Deep laser penetration loosens the contracture of full-thickness scars, and it increases tissue elasticity and the proportion of type III collagen in the scars, which mainly serves to restore the function of contracture scars. The mono-scan of LF–HD laser treatment did not show significant advantages over the control group. The main advantages of the combined group included the grinding of superficial tissue, reducing the small protrusions and restoring the flatness, which improved the cosmetic appearance.

This study used an excisional model instead of a burn model in red Duroc pigs in order to avoid interference due to differences in wound depth. The excisional model produced a scar thinner than that in the burn model, but was reported similar to that in humans [38–40]. Significant reduction of the scar area begins to occur 4–9 weeks after skin grafting of the porcine dorsum [41], and the time point of 42 days postoperative for the initial laser intervention was chosen for the early management of the contracture. Further clinical trials are needed to determine whether fractional laser should be used prophylactically at high-risk sites in clinical applications.

As a commonly used animal model for contracted skin grafts, red Duroc pigs provide a reference for the parameters of fractional CO_2 laser application in clinical practice. One limitation of this study is the small number of animals used. Although pigs of a similar age, sex and weight were selected, and individual differences were compared before the intervention and block randomization was used to avoid the effect of scar location, individual differences could not be completely excluded. More accurate parameter selection should be made with the help of prospective clinical trials with large samples. Laser penetration close to the full scar thickness was thought to produce higher scar release rates and further studies could explore the optimal depth of laser penetration in contracture scar treatment.

Downloaded from academic.oup.com/burnstrauma/article/doi/10.1093/burnst/tkab048/6490349 by guest on 14 October 2026

Conclusions

This study comprehensively describes a dual-scan protocol for fractional CO_2 laser in a red Duroc pig dorsal skin graft model and compares its effectiveness and safety with conventional mono-scan protocol. The results show that the dual-scan protocol could achieve superficial ablation and deep release of contracted skin graft in a single treatment, increasing scar release, elasticity and surface flatness. The contracture release and texture improvement were similar compared to the single deep scan, with the main advantage of restoring a smoother scar appearance and improving cosmetic outcome. Adequate laser penetration was necessary for the release of contracted scars.

Supplementary material

Supplementary material is available at *Burns & Trauma Journal* online.

Authors' contributions

YZ and WS designed the study; JL and JW conducted experiment and wrote the draft; ZZ and HL collected and analysed the data; WX and SKN revised the draft; XW performed the histological examination. All authors read and approved the final manuscript.

Funding

This study was supported by Shanghai Municipal Education Commission Gaofeng Clinical Medicine Grant Support (20152227); The national natural science foundation of China (81772098); Scientific research foundation of Shanghai Municipal Commission of Health and Family Planning (20154Y0023).

Ethics approval

All experimental operations were carried out and data were collected following the standards of the Animal Ethics Committee of the Shanghai Jiao Tong University School of Medicine.

Conflicts of interest

The authors declare that they have no competing interests.

Abbreviations

HF–LD: High fluence- low density; LF–HD: Low fluence-high density; H&E: Hemoglobin and eosin.

References

1. McDonald WS, Deitch EA. Hypertrophic skin grafts in burned patients: a prospective analysis of variables. *J Trauma*. 1987;27:147–50.
2. Schneider JC, Holavanahalli R, Helm P, Goldstein R, Kowalske K. Contractures in burn injury: defining the problem. *Journal of burn care & research: official publication of the American Burn Association*. 2006;27:508–14.
3. Harrison CA, MacNeil S. The mechanism of skin graft contraction: an update on current research and potential future therapies. *Burns*. 2008;34:153–63.
4. Schouten HJ, Nieuwenhuis MK, van Zuijlen PP. A review on static splinting therapy to prevent burn scar contracture: do clinical and experimental data warrant its clinical application? *Burns*. 2012;38:19–25.
5. Wiseman J, Ware RS, Simons M, McPhail S, Kimble R, Dotta A, *et al*. Effectiveness of topical silicone gel and pressure garment therapy for burn scar prevention and management in children: a randomized controlled trial. *Clin Rehabil*. 2020;34:120–31.
6. DeBruler DM, Zbinden JC, Baumann ME, Blackstone BN, Malara MM, Bailey JK, *et al*. Early cessation of pressure garment therapy results in scar contraction and thickening. *PLoS One*. 2018;13:e0197558. doi: 10.1371/journal.pone.0197558.
7. Shumaker PR, Kwan JM, Landers JT, Uebelhoer NS. Functional improvements in traumatic scars and scar contractures using an ablative fractional laser protocol. *J Trauma Acute Care Surg*. 2012;73:S116–21.
8. Lv K, Liu H, Xu H, Wang C, Zhu S, Lou X, *et al*. Ablative fractional CO (2) laser surgery improving sleep quality, pain and pruritus in adult hypertrophic scar patients: a prospective cohort study. *Burns & trauma*. 2021;9:tkab023.
9. Dai Z, Lou X, Shen T, Sun Y, Xiao Y, Zheng X, *et al*. Combination of ablative fractional carbon dioxide laser and platelet-rich plasma treatment to improve hypertrophic scars: a retrospective clinical observational study. *Burns Trauma*. 2021;9:tkab016. doi: 10.1093/burnst/tkab016.
10. Kroonen L, Shumaker PR, Kwan JM, Uebelhoer N, Hofmeister E. Treatment of split-thickness skin graft-related forearm scar contractures with a carbon dioxide laser protocol: 3 case reports. *J Hand Surg Am*. 2013;38:2164–8.
11. Krakowski AC, Goldenberg A, Eichenfield LF, Murray JP, Shumaker PR. Ablative fractional laser resurfacing helps treat restrictive pediatric scar contractures. *Pediatrics*. 2014;134:e1700–5.
12. Zuccaro J, Ziolkowski N, Fish J. A systematic review of the effectiveness of laser therapy for hypertrophic burn scars. *Clin Plast Surg*. 2017;44:767–79.
13. Kucukkaya D, Irkoren S, Ozkan S, Sivrioglu N. The effects of botulinum toxin a on the wound and skin graft contraction. *J Craniofac Surg*. 2014;25:1908–11.
14. Kwak M, Son D, Kim J, Han K. Static Langer's line and wound contraction rates according to anatomical regions in a porcine model. *Wound Repair Regen*. 2014;22:678–82.
15. DeBruler DM, Blackstone BN, Baumann ME, McFarland KL, Wulff BC, Wilgus TA, *et al*. Inflammatory responses, matrix remodeling, and re-epithelialization after fractional CO2 laser treatment of scars. *Lasers Surg Med*. 2017;49:675–85.
16. Kanapathy M, Mosahebi A. Comparative study on the donor site aesthetic outcome between epidermal graft and split-thickness skin graft. *Int Wound J*. 2019;16:354–9.
17. Klifto KM, Asif M, Hultman CS. Laser management of hypertrophic burn scars: a comprehensive review. *Burns Trauma*. 2020;8:tkz002. doi: 10.1093/burnst/tkz002.
18. Baumann ME, Blackstone BN, Malara MM, Clairmonte IA, Supp DM, Bailey JK, *et al*. Fractional CO2 laser ablation

Downloaded from academic.oup.com/burnstrauma/article/doi/10.1093/burnst/tkab048/6490349 by guest on 14 October 2026

of porcine burn scars after grafting: is deeper better? *Burns*. 2020;46:937–48.
19. Anderson RR, Donelan MB, Hivnor C, Greeson E, Ross EV, Shumaker PR, *et al*. Laser treatment of traumatic scars with an emphasis on ablative fractional laser resurfacing: consensus report. *JAMA Dermatol*. 2014;150:187–93.
20. Yuan XH, Zhong SX, Li SS. Comparison study of fractional carbon dioxide laser resurfacing using different fluences and densities for acne scars in Asians: a randomized split-face trial. *Dermatol Surg*. 2014;40:545–52.
21. Tierney EP. Treatment of acne scarring using a dual-spot-size ablative fractionated carbon dioxide laser: review of the literature. *Dermatol Surg*. 2011;37:945–61.
22. Poetschke J, Dornseifer U, Clementoni MT, Reinholz M, Schwaiger H, Steckmeier S, *et al*. Ultrapulsed fractional ablative carbon dioxide laser treatment of hypertrophic burn scars: evaluation of an in-patient controlled, standardized treatment approach. *Lasers Med Sci*. 2017;32:1031–40.
23. Kotlus BS. Dual-depth fractional carbon dioxide laser resurfacing for periocular rhytidosis. *Dermatol Surg*. 2010;36: 623–8.
24. Hultman CS, Friedstat JS, Edkins RE, Cairns BA, Meyer AA. Laser resurfacing and remodeling of hypertrophic burn scars: the results of a large, prospective, before-after cohort study, with long-term follow-up. *Ann Surg*. 2014;260:519–29 discussion 529-532.
25. Issler-Fisher AC, Fisher OM, Haertsch P, Li Z, Maitz PKM. Ablative fractional resurfacing with laser-facilitated steroid delivery for burn scar management: does the depth of laser penetration matter? *Lasers Surg Med*. 2020;52:149–58.
26. Lee SJ, Suh DH, Lee JM, Song KY, Ryu HJ. Dermal Remodeling of burn scar by fractional CO2 laser. *Aesthetic Plast Surg*. 2016;40:761–8.
27. Xie CH, Gao XX, Meng XL, Chen KX, Zhang XH, Zhou X, *et al*. Effect analysis of sequential laser application in treating the hypertrophic scars of burn children at early stage. *Chin J Burns*. 2021;37:327–32.
28. Ozog DM, Liu A, Chaffins ML, Ormsby AH, Fincher EF, Chipps LK, *et al*. Evaluation of clinical results, histological architecture, and collagen expression following treatment of mature burn scars with a fractional carbon dioxide laser. *JAMA Dermatol*. 2013;149:50–7.
29. Cho SB, Lee SJ, Kang JM, Kim YK, Kim TY, Kim DH. The treatment of burn scar-induced contracture with the pinhole method and collagen induction therapy: a case report. *J Eur Acad Dermatol Venereol*. 2008;22:513–4.
30. Tierney EP, Hanke CW, Watkins L. Treatment of lower eyelid rhytids and laxity with ablative fractionated carbon-dioxide laser resurfacing: case series and review of the literature. *J Am Acad Dermatol*. 2011;64:730–40.
31. Datz E, Schonberger C, Zeman F, Koller M, Berneburg M, Landthaler M, *et al*. Fractional carbon dioxide laser resurfacing of skin grafts: long-term results of a prospective, randomized, split-scar, evaluator-blinded study. *Lasers Surg Med*. 2018;50:1010–6.
32. Avram MM, Tope WD, Yu T, Szachowicz E, Nelson JS. Hypertrophic scarring of the neck following ablative fractional carbon dioxide laser resurfacing. *Lasers Surg Med*. 2009;41:185–8.
33. Karmisholt KE, Taudorf EH, Wulff CB, Wenande E, Philipsen PA, Haedersdal M. Fractional CO(2) laser treatment of caesarean section scars-a randomized controlled split-scar trial with long term follow-up assessment. *Lasers Surg Med*. 2017;49:189–97.
34. Cho SB, Lee SJ, Cho S, Oh SH, Chung WS, Kang JM, *et al*. Nonablative 1550-nm erbium-glass and ablative 10 600-nm carbon dioxide fractional lasers for acne scars: a randomized split-face study with blinded response evaluation. *J Eur Acad Dermatol Venereol*. 2010;24:921–5.
35. Huang L. A new modality for fractional CO2 laser resurfacing for acne scars in Asians. *Lasers Med Sci*. 2013;28:627–32.
36. Cameli N, Mariano M, Serio M, Ardigò M. Preliminary comparison of fractional laser with fractional laser plus radiofrequency for the treatment of acne scars and photoaging. *Dermatol Surg*. 2014;40:553–61.
37. Fitzpatrick RE, Smith SR, Sriprachya-anunt S. Depth of vaporization and the effect of pulse stacking with a high-energy, pulsed carbon dioxide laser. *J Am Acad Dermatol*. 1999;40:615–22.
38. Blackstone BN, Kim JY, McFarland KL, Sen CK, Supp DM, Bailey JK, *et al*. Scar formation following excisional and burn injuries in a red Duroc pig model. *Wound Repair Regen*. 2017;25:618–31.
39. Gallant CL, Olson ME, Hart DA. Molecular, histologic, and gross phenotype of skin wound healing in red Duroc pigs reveals an abnormal healing phenotype of hypercontracted, hyperpigmented scarring. *Wound Repair Regen*. 2004;12:305–19.
40. Zhu KQ, Carrougher GJ, Gibran NS, Isik FF, Engrav LH. Review of the female Duroc/Yorkshire pig model of human fibroproliferative scarring. *Wound Repair Regen*. 2007;15Suppl 1:S32–9.
41. DeBruler DM, Blackstone BN, McFarland KL, Baumann ME, Supp DM, Bailey JK, *et al*. Effect of skin graft thickness on scar development in a porcine burn model. *Burns*. 2018;44:917–30.

Downloaded from academic.oup.com/burnstrauma/article/doi/10.1093/burnst/tkab048/6490349 by guest on 14 October 2026